Results in Physics 27 (2021) 104517

Contents lists available at ScienceDirect

Results in Physics

journal homepage: www.elsevier.com/locate/rinp

Physically significant wave solutions to the Riemann wave equations and the Landau-Ginsburg-Higgs equation

Hemonta Kumar Barman [a], Most. Shewly Aktar [b], M. Hafiz Uddin [c], M. Ali Akbar [d,*], Dumitru Baleanu [e,f,g], M.S. Osman [h,i]

[a] Department of Computer Science and Engineering, University of Creative Technology Chittagong, Bangladesh
[b] Department of Electrical and Electronic Engineering, Varendra University, Bangladesh
[c] Department of Mathematics, Jashore University of Science and Technology, Bangladesh
[d] Department of Applied Mathematics, University of Rajshahi, Bangladesh
[e] Department of Mathematics, Cankaya University, 06530 Ankara, Turkey
[f] Institute of Space Sciences, Magurele, 077125 Bucharest, Romania
[g] Department of Medical Research, China Medical University Hospital, China Medical University, Taichung, Taiwan
[h] Department of Mathematics, Faculty of Science, Cairo University, Giza 12613, Egypt
[i] Department of Mathematics, Faculty of Applied Science, Umm Alqura University, Makkah 21955, Saudi Arabia

ARTICLE INFO

Keywords:
Riemann wave equations
Landau-Ginsburg-Higgs equation
The extended tanh-function scheme
Solitary wave solutions

ABSTRACT

The nonlinear Riemann wave equations (RWEs) and the Landau-Ginsburg-Higgs (LGH) equation are related to plasma electrostatic waves, ion-cyclotron wave electrostatic potential, superconductivity, and drift coherent ion-cyclotron waves in centrifugally inhomogeneous plasma. In this article, the interactions between the maximum order linear and nonlinear factors are balanced to compute realistic soliton solutions to the formerly stated equations in terms of hyperbolic functions. The linear and nonlinear effects rheostat the structure of the wave profiles, which vary in response to changes in the subjective parameters combined with the solutions. The established solutions to the aforementioned models using the extended tanh scheme are descriptive, typical, and consistent, and include standard soliton shapes such as bright soliton, dark soliton, compacton, peakon, periodic, and others that can be used to analyze in ion-acoustic and magneto-sound waves in plasma, homogeneous, and stationary media, particularly in the propagation of tidal and tsunami waves.

Introduction

The studies of the nonlinear wave equations (NLWEs) have developed steadily with notable advancement over many decades. These equations raised in nonlinear science, mathematical physics, and engineering have significant properties to describe nonlinear wave incidents such as dispersion, dissipation, diffusion, reaction, convection, etc [1–5]. Because of the accessibility of the typical computation frameworks Maple and Mathematica, which empower us to perform complex computations on computers, the study of exact traveling wave solutions for NLWEs has immersed sensibly these days to disclose these properties. Besides, traveling waves appear with physical characteristics in solitary wave theory such as bell-shaped solitons, kink, peakon, cuspon, compactons, periodic, complexiton, positon, negaton, etc. Indeed, solitons are localized traveling waves that are asymptotically zero at great distances. For integrable models, the interactions between soliton solutions are fully elastic. Here, elastic interaction means that if a soliton collides with another similar soliton, they interact behind losing their own identities. That is, after a nonlinear interaction, a soliton's amplitude, velocity, and waveform remain unaffected. However, in some soliton models, when unique conditions between the wave trajectories and velocities are fulfilled, such as in compactons, fully non-elastic interactions can occur. For real-world physical models, one can find soliton phenomena in organic membrane and macromolecule materials, SrBaNi oxidation crystal and waveguide, even-clump DNA, shallow water waves, matter waves in Bose-Einstein condensates, surface manifestations of internal gravity waves, ultrashort pulses in nonlinear optics, signal processing in optical fiber, geophysics, plasma physics, nuclear physics, hydrodynamics, etc. [6–8]. Because of this, numerous analysts have developed different techniques [9–32] for tracing soliton

* Corresponding author.
E-mail address: ali_math74@yahoo.com (M.A. Akbar).

https://doi.org/10.1016/j.rinp.2021.104517
Received 5 May 2021; Received in revised form 18 June 2021; Accepted 1 July 2021
Available online 6 July 2021

solutions, each of which has its own set of constraints, arising for the advancement of existing schemes or the require for new techniques. In this regard, the present paper examines the solitary wave profiles of two distinct classes of integrable NLWEs of any order. The (2 + 1)-dimensional generalized breaking soliton equation was proposed in the form [33]:

$$U_t + aU_{xxx} + bU_{xxy} + cUU_x + dUU_y + eU_x\partial_x^{-1}U_y = 0 \tag{1}$$

where about *a, b, c, d, e* are real parameters. Eq. (1) indicates that it has the Painleve property for the parametric choice $a = 0$ by applying singularity structure analysis [34]. The unique property of the family of these equations is that the spectral parameter availed in the Lax representations exhibits the breaking behavior. The spectral value thus develops a multivalued function. As a result, the solution of these equations can also turn into multivalued. In consequence, Eq. (1) is connected to the (2 + 1)-dimensional breaking soliton equations [34]:

$$U_t + aU_{xxx} + bU_{xxy} + cUU_x + dUW_x + eU_xW = 0 \tag{2a}$$

$$U_y = W_x \tag{2b}$$

Eqs. (2a) and (2b) were first thoroughly investigated where overlapping solutions were evaluated [35]. Moreover, Eqs. (2a) and (2b) have many special classes of NLWEs as explained by Xu [36]. In what follows, we study the Riemann wave model of the form [37]:

$$U_t + lU_{xxy} + mUW_x + nU_xW = 0 \tag{3a}$$

$$U_y = W_x \tag{3b}$$

where *l*, *m*, and *n* are nonzero parameters. Eqs. (3a) and (3b) describe the (2 + 1)-dimensional interaction of the Riemann wave propagating along the *y*-axis with a long wave along the *x*-axis. These equations are fully integrable and have numerous applications in the propagation of ocean tsunamis and tidal waves. Another important feature of the equations (3a) and (b) is the representation of the turbulent state by the combination of the whistle wave packets with the finite-amplitude random phases. The Whistler turbulence interacts with the magnetic-sound wave, resulting in the damping of the latter which dampens the electrostatic wave in the plasma [38].

On the contrary, a new class of nonlinear evolution equations (NLEEs) with a nonlinear term of any order [39] is of the form

$$U_{tt} + a_1U_{xx} + a_2U + a_3U^p + a_4U^{2p-1} = 0 \tag{4}$$

where a_1, a_2, a_3, a_4, and $p \neq 1$ are all arbitrary constants. When p is changed to a different constant, a new equation is formed. The special case of the NLEEs [40] when $p = 3, a_4 = 0$ is stated as

$$U_{tt} + \alpha U_{xx} + \beta U + \gamma U^3 = 0 \tag{5}$$

A typical form of the NLEE (5) is specified as the LGH equation [41,42]

$$U_{tt} - U_{xx} - a^2U + b^2U^3 = 0 \tag{6}$$

where $U(x, t)$ defines the ion-cyclotron wave electrostatic potential, a and b are real parameters, and x, $t$denote the spatial and temporal coordinates. The LGH Eq. (6) was developed by Landau and Ginzburg for interpreting superconductivity and drift cyclotron waves in centrifugally inhomogeneous plasma for coherent ion-cyclotron waves [43].

Searching for explicit solutions to both RWEs (3a) and (3b) and the LGH equation (6) using a variety of approach is a crucial part of mathematical physics, and it has recently become as the most fascinating and exciting subject of study. When studying the physical processes of natural phenomena characterized by RWEs and LGH equations, the exact solutions to these equations should be investigated. There are a few typical schemes to find exact solutions to the integrable RWEs as well as the LGH equations in the literature [44–60]. Therefore, we aim in the present article to establish inclusive, standard, significant and comprehensible soliton structured solutions to the RWEs and the LGH equation that are localized in all directions of (2 + 1)-dimensions utilizing the extended tanh-function procedure [61,62], where a finite power series in tanh is used as an ansatz.

The layout of this article is arranged in the ensuing paragraphs: In paragraph 2, we present succinctly the extended tanh function technique. In paragraph 3, the exact solutions of the considered NLWEs are established. In paragraph 4, graphical depictions and physical explanations are provided. In paragraph 5, we compare the obtained solutions with the solutions existing in the literature. Finally, the conclusion of this article has been drawn.

Overview of the extended tanh-function technique

This section describes the extended tanh function technique for obtaining ample exact solutions for NLWEs. The core idea behind this process is to express the solution as a polynomial in hyperbolic functions, and then to solve a system of algebraic equations implies to solve the corresponding NLWEs. To start with, we apprehend an NLWE built in a function $U = U(x, y, t)$ of the form

$$S\left(U_t, U_{xt}, U_{xx}, U_{tt}, U_{xyt}, \cdots\right) = 0 \tag{7}$$

wherein the function $U = U(x, t)$ is to be evaluated, S is a polynomial of the unknown variable U and also its derivatives, $U_t, U_{xt}, U_{xx}, U_{tt}, U_{xyt}$, $\cdots$ in space and time coordinates.

A new transformation, name wave variable

$$U(x, y, t) = U(\lambda), \lambda = gx + hy - ct \tag{8}$$

where $U(\lambda)$ embodies the localized wave solutions traveling at speed c, and g, h define the wavenumbers, modifies (7) into the ensuing nonlinear differential equation

$$R(U^{'}, U^{''}, U^{'''}, \cdots) = 0 \tag{9}$$

Now, we consider a formal solution structure of Eq. (9) in the following

$$U(\lambda) = \sum_{j=0}^{M} p_jZ^j + \sum_{j=1}^{M} q_jZ^{-j} \tag{10}$$

wherein

$$Z = \tanh(k\lambda) \tag{11}$$

and k is an arbitrary constant. In Eq. (9), the highest derivative and nonlinear term yield the balance number M.

Introducing solution (10) along with Eq. (11) into Eq. (9), a polynomial in $Z(\lambda)$ is a consequence. A series of algebraic equations for $p_j (j = 0, 1, 2, \cdots, M)$ and $q_j (j = 1, 2, \cdots, M)$ is obtained by setting each coefficient of the resultant polynomials to zero. Finally, the required solutions through the values of $p_j (j = 0, 1, 2, \cdots, M)$ and $q_j (j = 1, 2, \cdots, M)$ will be determined.

Analysis of solutions

This module constructs the extended tanh function scheme for establishing the traveling wave solutions to the Riemann wave equations and the Landau-Ginsburg-Higgs equation.

The Riemann wave equations

The RWEs (3a) and (3b) are considered in this sub-module in order to develop advanced and broad-spectrum solitary wave solutions. The wave variable (8) remodels the Eqs. (3a) and (3b) into the following system

$$hlg^2U''' + mgUW' + nWU' = 0 \tag{12}$$

$$hU' = gW' \tag{13}$$

Eq. (13) has been integrated considering zero integration constant, thus it is found

$$W = (h/g)U \tag{14}$$

Replacing W and W' in Eq. (12) provide the subsequent nonlinear equation

$$hlg^2U''' + h(m+n)UU' - 2cU' = 0 \tag{15}$$

Integrating and omitting the integration constant yields

$$2hlg^2U'' + h(m+n)U^2 - 2cU = 0 \tag{16}$$

By leveling the highest derivative and nonlinear term occupied in Eq. (16), the index number $M = 2$ is revealed from which a particular form of Eq. (10) can be set as

$$U(\lambda) = p_0 + p_1Z + p_2Z^2 + q_1Z^{-1} + q_2Z^{-2} \tag{17}$$

wherein p_0, p_1, p_2, q_1 and q_2 are the arbitrary constants to be calculated. Placing the solution (17) together with equation (11) into Eq. (16) leads to a nonlinear system in terms of $Z(\lambda)$. Then after equating the coefficient of $Z(\lambda)$ and setting them to zero, a certain nonlinear system of algebraic equations is generated below:

$$Z(\lambda)^0 : hq_2\left(12lg^2k^2 + mq_2 + nq_2\right) = 0 \tag{18}$$

$$Z(\lambda)^1 : 2hq_1\left(2lg^2k^2 + mq_2 + nq_2\right) = 0 \tag{19}$$

$$Z(\lambda)^2 : \left(\left(2p_0q_2 + q_1{}^2\right)m + \left(2p_0q_2 + q_1{}^2\right)n - 16q_2lg^2k^2\right)h - 2cq_2 = 0 \tag{20}$$

$$Z(\lambda)^3 : \left(\left(2p_0q_1 + 2p_1q_2\right)m + \left(2p_0q_1 + 2p_1q_2\right)n - 4q_1lg^2k^2\right)h - 2cq_1 = 0 \tag{21}$$

$$Z(\lambda)^4 : \left(\left(p_0{}^2 + 2p_1q_1 + 2p_2q_2\right)m + \left(p_0{}^2 + 2p_1q_1 + 2p_2q_2\right)n + 4lg^2k^2(p_2 + q_2)\right)h - 2ca_0 = 0 \tag{22}$$

$$Z(\lambda)^5 : \left(\left(2p_0p_1 + 2p_2q_1\right)m + \left(2p_0p_1 + 2p_2q_1\right)n - 4p_1lg^2k^2\right)h - 2cp_1 = 0 \tag{23}$$

$$Z(\lambda)^6 : \left(\left(2p_0p_2 + p_1{}^2\right)m + \left(2p_0p_2 + p_1{}^2\right)n - 16p_2lg^2k^2\right)h - 2cp_2 = 0 \tag{24}$$

$$Z(\lambda)^7 : 2hp_1\left(2lg^2k^2 + mp_2 + np_2\right) = 0 \tag{25}$$

$$Z(\lambda)^8 : hp_2\left(2lg^2k^2 + mp_2 + np_2\right) = 0 \tag{26}$$

Different ramifications of solutions are obtained as a result of solving the above nonlinear system of algebraic equations:

Cluster 1

$c = -16hlg^2k^2$, $p_0 = -\frac{8lg^2k^2}{m+n}$, $p_1 = q_1 = 0$, $p_2 = -\frac{12lg^2k^2}{m+n}$, $q_2 = -\frac{12lg^2k^2}{m+n}$.

The values of the parameters available in Cluster 1 constitute an explicit solution in terms of tanh and coth functions

$$U(\lambda) = -\frac{lg^2k^2}{m+n}\left(8 + 12\tanh^2(k\lambda) + 12\coth^2(k\lambda)\right) \tag{27}$$

which can be reconstructed using the hyperbolic formula with respect to space and time coordinates

$$U(x,y,t) = -\frac{lg^2k^2}{m+n}\left(8 + 12\tanh^2(k(gx+hy-ct)) + 12\coth^2(k(gx+hy-ct))\right) \tag{28}$$

The similar solution (14), on the other hand, becomes

$$W(x,y,t) = -\frac{hlgk^2}{m+n}\left(8 + 12\tanh^2(k(gx+hy-ct)) + 12\coth^2(k(gx+hy-ct))\right) \tag{29}$$

Cluster 2

$c = 4hlg^2k^2$, $p_0 = \frac{12lg^2k^2}{m+n}$, $p_2 = -\frac{12lg^2k^2}{m+n}$, $p_1 = q_1 = q_2 = 0$.

The values of the parameters presented in Cluster 2 generates an explicit bell-shaped soliton solution concerning sech function

$$U(x,y,t) = \frac{12lg^2k^2}{m+n}\mathrm{sech}^2(k(gx+hy-ct)) \tag{30}$$

Another respective solution (14) becomes

$$W(x,y,t) = \frac{12hlgk^2}{m+n}\mathrm{sech}^2(k(gx+hy-ct)) \tag{31}$$

Cluster 3

$c = -4hlg^2k^2$, $p_0 = \frac{4lg^2k^2}{m+n}$, $p_2 = -\frac{12lg^2k^2}{m+n}$, $p_1 = q_1 = q_2 = 0$.

The values of the parameters presented in Cluster 3 put together another closed solution regarding sech functions

$$U(x,y,t) = -\frac{lg^2k^2}{m+n}\left(8 - 12\mathrm{sech}^2(k(gx+hy-ct))\right) \tag{32}$$

And the pair solution (14) turns into

$$W(x,y,t) = -\frac{hlgk^2}{m+n}\left(8 - 12\mathrm{sech}^2(k(gx+hy-ct))\right) \tag{33}$$

Cluster 4

$c = 16hlg^2k^2$, $p_0 = \frac{24lg^2k^2}{m+n}$, $p_1 = q_1 = 0$, $p_2 = -\frac{12lg^2k^2}{m+n}$, $q_2 = -\frac{12lg^2k^2}{m+n}$.

On the other hand, introducing the values of the constraints gathered in Cluster 4 into (17), it can be found solution for $U(x,y,t)$ that is comparable to solution (28). And, based on (14), the solution for $W(x,y,t)$ is comparable to solution (29). There is just a variation in constant, which does not alter the profile of any wave but only translocate it. Thus, the solutions have not been written for the values in Cluster 4.

Cluster 5

$c = -4hlg^2k^2$, $p_0 = \frac{4lg^2k^2}{m+n}$, $p_1 = p_2 = q_1 = 0$, $q_2 = -\frac{12lg^2k^2}{m+n}$.

The values of the parameters obtained in Cluster 5 form a different explicit solution in terms of coth function

$$U(x,y,t) = \frac{lg^2k^2}{m+n}\left(4 - 12\coth^2(k(gx+hy-ct))\right) \tag{34}$$

The solution (14) then changes to

$$W(x,y,t) = \frac{hlgk^2}{m+n}\left(4 - 12\coth^2(k(gx+hy-ct))\right) \tag{35}$$

Cluster 6

$c = 4hlg^2k^2$, $p_0 = \frac{12lg^2k^2}{m+n}$, $p_1 = p_2 = q_1 = 0$, $q_2 = -\frac{12lg^2k^2}{m+n}$.

Furthermore, placing the parameter values involved in Cluster 6 to (17) yields a solution of $U(x,y,t)$ that is equivalent to the solution (32). Besides, the solution of $W(x,y,t)$ based on (14) is equivalent to the solution (33). There is just a difference in constant that does not affect the profile of any wave, but merely translates it. Therefore, the solutions are written for the values of Cluster 6.

The Landau-Ginsburg-Higgs equation

In this parameter, the LGH model (6) will be investigated to ascertain advanced and inclusive solitary wave solutions. The wave variable defined by

$$U(x,t) = U(\lambda), \lambda = \beta x - ct \tag{36}$$

remodels the LGH (6) into the ensuing equation

$$\left(c^2 - \beta^2\right)U'' - a^2U + b^2U^3 = 0 \tag{37}$$

The balancing principle in Eq. (35) provides the index number $M = 1$. As a result, finite series (10) becomes the subsequent form

$$U(\lambda) = p_0 + p_1Z + q_1Z^{-1} \tag{38}$$

where p_0, p_1 and q_1 be the unrevealed constants to be evaluated. Embedding the solution (38) together with (11) into Eq. (37) provides a nonlinear system in terms of $Z(\lambda)$ to be zero.

$$2k^2c^2q_1 - 2k^2\beta^2q_1 + b^2{q_1}^3 = 0 \tag{39}$$

$$3b^2p_0{q_1}^2 = 0 \tag{40}$$

$$-2k^2c^2q_1 + 2k^2\beta^2q_1 - a^2q_1 + 3b^2{p_0}^2q_1 + 3b^2p_1{q_1}^2 = 0 \tag{41}$$

$$-p_0a^2 + b^2{p_0}^3 + 6b^2p_0p_1q_1 = 0 \tag{42}$$

$$-2k^2c^2p_1 + 2k^2\beta^2p_1 - p_1a^2 + 3b^2{p_0}^2p_1 + 3b^2{p_1}^2q_1 = 0 \tag{43}$$

$$3b^2p_0{p_1}^2 = 0 \tag{44}$$

$$2k^2c^2p_1 - 2k^2\beta^2p_1 + b^2{p_1}^3 = 0 \tag{45}$$

The above nonlinear system of algebraic equations provides solutions separated into some clusters given in the underneath:

Cluster 1

$c = \pm\frac{\sqrt{4k^2\beta^2-2a^2}}{2k}$, $p_1 = \pm\frac{a}{b}$, $p_0 = q_1 = 0$.

For evaluating the exact solution, we insert the values of the parameters in solution (38) and achieve the tanh function solution of the form

$$U(\lambda) = \pm\frac{a}{b}\tanh(k\lambda) \tag{46}$$

which can be outlined in terms of space and time coordinates

$$U(x,t) = \pm\frac{a}{b}\tanh(k(\beta x - ct)) \tag{47}$$

Cluster 2

$c = \pm\frac{\sqrt{6k^2\beta^2-2a^2}}{4k}$, $p_0 = 0$, $p_1 = q_1 = \pm\frac{0.5a}{b}$.

Placing the values of the unspecified parameters in solution (38) reveal an exact solution with the combination of tanh and coth functions

$$U(x,t) = \pm\frac{0.5a}{b}(\tanh(k(\beta x - ct)) + \coth(k(\beta x - ct))) \tag{48}$$

Cluster 3

$c = \pm\frac{\sqrt{4k^2\beta^2+a^2}}{2k}$, $p_0 = 0$, $p_1 = q_1 = \pm\frac{\sqrt{-0.5}a}{b}$.

Inserting the values of the unspecified parameters in solution (38) formulate the ensuing solution in terms of tanh and coth function

$$U(x,t) = \pm\frac{\sqrt{-0.5}a}{b}(\tanh(k(\beta x - ct)) + \coth(k(\beta x - ct))) \tag{49}$$

Wave profile analysis

This section consisting of two subsections addresses the graphical representations and discussions of numerous solitary waves of the determined solutions to the RWEs and LGH equation. Several forms of 3D and contour surfaces are represented using the mathematical symbolic computation program Wolfram Mathematica by taking appropriate values of the unspecified parameters to contemplate the mechanism of physic illustrated by the RWEs and LGH equations. Here, the contour profile is used to investigate the wave nature and how various parameters affect the transformation of three-dimensional wave profiles into two-dimensional plots. One variable, x, is chosen on the horizontal axis, and the second variable, y, is chosen on the vertical axis, to create a contour map. The third variable z, is represented by a color gradient and isolines. These graphs are frequently used in data analysis, particularly when searching for the highest and lowest in a set of trivariate data.

The wave profile of the RWEs

It is crucial to note that the characteristics of the wave profiles are determined by the values of the existing parameters in the RWEs. To illustrate the point, different depictions of the solution functions (27)-(35) are drawn for some definite values of c, m and n, where the free parameters l, g, h, k affect the wave velocity c, and the parameters l, g, h, m, n are related to the coefficient of the greatest power of the linear and nonlinear terms of Eq. (16). We draw the steady propagation of all the solitary wave findings in this article for RWEs in x and y coordinate only due to the difficulty in drawing $(2+1)$-dimensional shapes in 3D and contour maps. The solution $U(x,y)$ obtained in (28) signifies a flat parabolic soliton for $g = -2, h = -0.21, k = -0.23, l = m = n = -2$ presented in 3D as well as contour into the range $2 \le x,y \le 7$ shown in Fig. 1(a). By increasing the values $g = -0.01, k = 0.09$, decreasing $h = -1.41$, choosing positive $l = 0.64$, and unchanging m, n, the solution $W(x,y)$ in (29) depicts also a flat parabolic soliton apparent in the 3D unchanged spatial and the contour as portrayed in Fig. 1(b).

The solutions (30) and (31), on the other hand, describe the other shapes induced by considering another specific value of the wave velocity c which is determined by allocating the parameters g, h, as well as the coefficient l of the linear factor in Eq. (16) randomly. For the values $g = 0.22, h = -0.21, k = l = m = n = -2$, the solution $U(x,y)$ results as in smooth bright soliton delineated in Fig. 2(a). While decreasing the values of the free parameter $g = -0.27, h = -0.23$, increasing $l = 0.87$ and keeping k, m, n, unchanged, the pair solution $W(x,y)$ reflects the identical propagation of this shape when displaced from its original location and converts to the smooth bright soliton which is outlined in Fig. 2(b). The boundary $-5 \le x,y \le 5$, is chosen both for 3D and contour figures.

It is notable that the solution functions (32) and (33) demonstrate another identity of the solitary waves with compact support. The solution $U(x,y)$ shows the compacton wave for choosing the positive $h = 0.11, k = 0.03$ and the negative $g = -0.12, l = m = n = -2$. Likewise, the pair solution $W(x,y)$ also produces the compacton for choosing only positive $g = 0.09$ and all negative $h = -0.08, k = -0.16, l = -1.62$, $m = n = -2$. These indicate that the location of the figure can be shifted, compressed, or stretched simply by changing the value of the weight k, the coefficient of the linear term, and the wavenumbers that

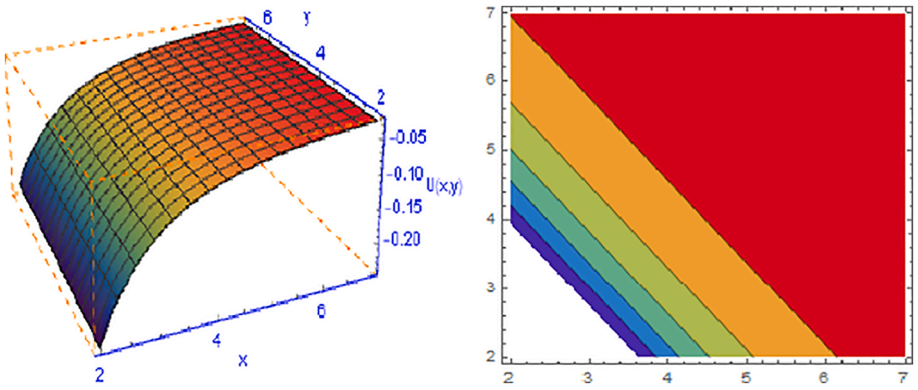

Fig. 1a. Flat parabolic wave of solution (28) for $g = -0.63$, $h = -0.01$, $k = 0.09$, $l = -0.33$,$m = n = -2$

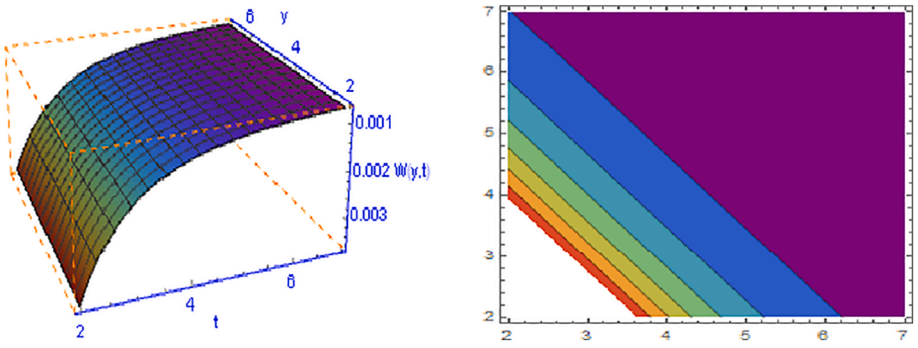

Fig. 1b. Flat parabolic wave of (29) for $g = -0.01$, $h = -1.41$, $k = 0.09$, $l = 0.64$, $m = \mathrm{n} = -2$.

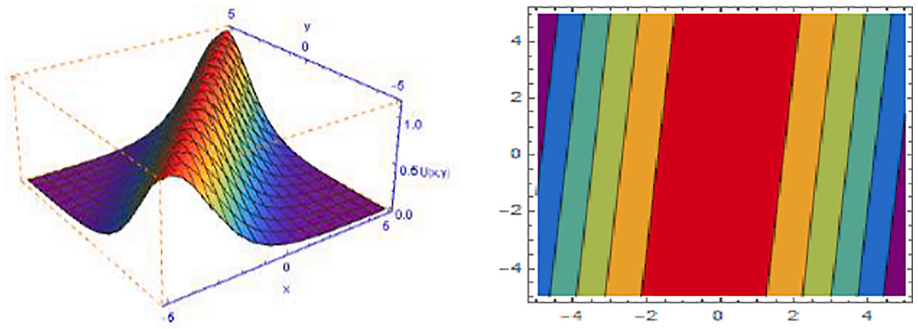

Fig. 2a. Propagation of bright solitary wave solution (30) for.$g = 0.22, h = -0.21, k = l = m = n = -2$

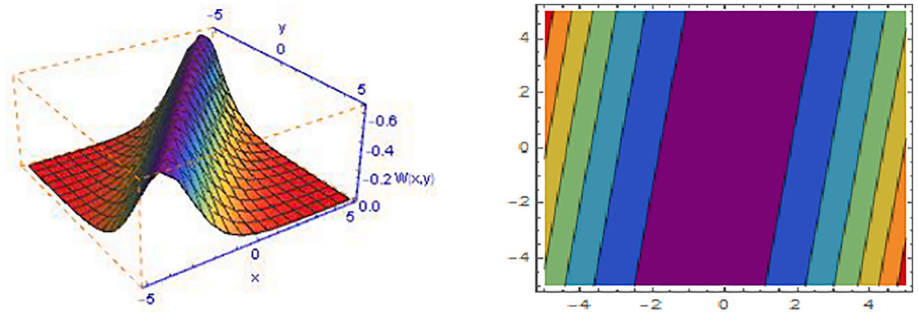

Fig. 2b. Propagation of bright solitary wave solution (31) for.$g = -0.27, h = -0.23, l = 0.87, k = m = n = -2$

produce the wave's speed velocity c with finite wavelength and compact support. The 3D and contour profiles have been depicted in Figs. 3(a) and 3(b) respectively within the limit $-20 \leq x,\ y \leq 20$. It is characterized by the absence of the exponential wings, wherein $U(\lambda)$, λ depends on x, y, and t in Eq. (8) does not tend to zero as $\lambda \to \infty$. The analysis of compactons will show a variety of nonlinear events, such as a

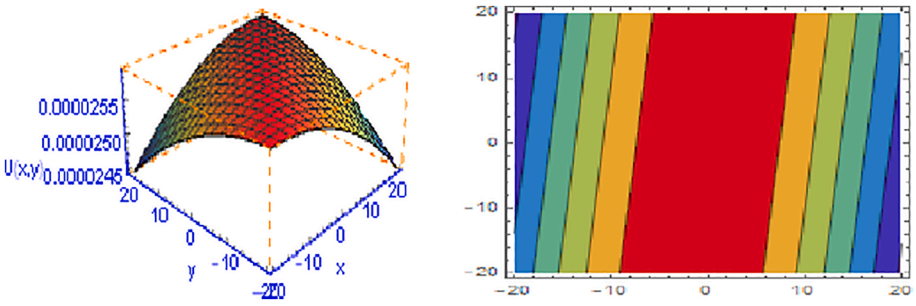

Fig. 3a. Plot of compacton solution (32) for $g = -0.12, h = 0.11, k = 0.03, l = m = n = -2$.

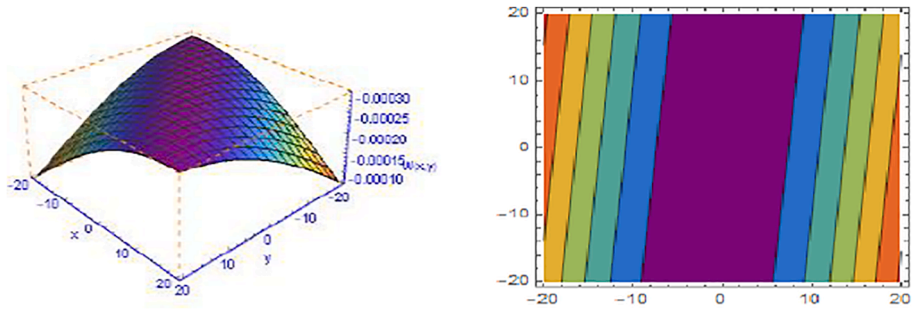

Fig. 3b. Plot of compacton solution (33) for $g = 0.09, h = -0.08, k = -0.16, l = -1.62, m = n = -2$.

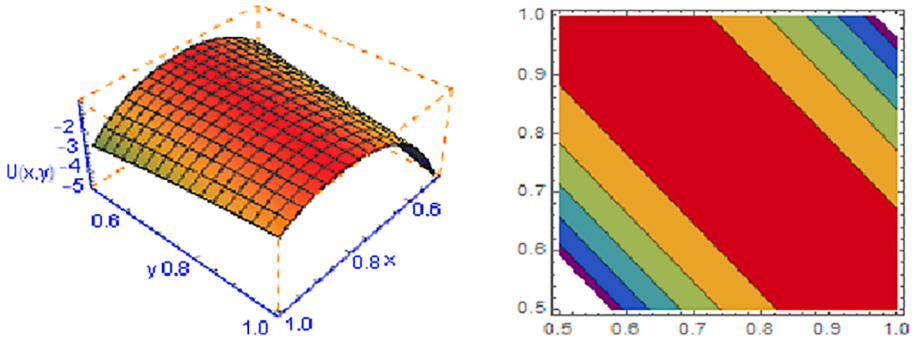

Fig. 4a. Trace of parabolic wave of solution (34) for $g = 1.2, h = -0.21, k = -0.21, l = 0.24, m = n = -2$.

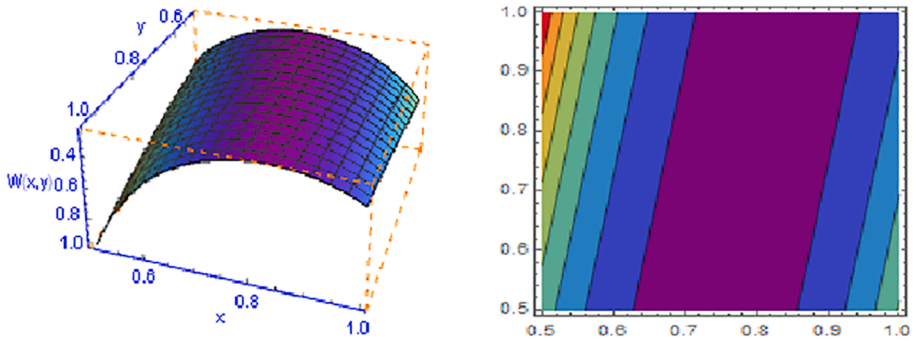

Fig. 4b. Trace of parabolic wave of solution (35) for $g = 1.2, h = -0.21, k = -2, l = 0.24, m = n = -2$.

cluster's hydrodynamic model, liquid drop fission and fusion mechanisms, super-deformed nuclei, etc.

For different values of the parameters related to the solutions (34) and (35), we attain parabolic shapes for both $U(x,y)$ and $W(x,y)$. If the values of the parameters $g = 1.2, h = -0.21, k = -0.21, l = 0.24, m = n = -2$, the solution $U(x,y)$ classifies a parabolic solitary wave and with the same value of g, h, l, m, n but different $k = -2$, the solution $W(x,y)$ implies alike parabolic solitary wave exposed by 3D and contour maps confined by $0 < x, y \leq 1$ in Figs. 4(a) and 4(b) respectively.

Based on the above investigation, it is noted that we have identified a variety of waveforms to the RWEs, including bell-shaped soliton, parabolic, flat parabolic, compacton, etc. Besides, we have examined how

the obtained solutions changed the nature of the waves produced and exposed that the coefficient of the utmost power of the linear and nonlinear terms of Eq. (16) has a great influence on the wave structures. Thus, accepting several values of l, g, h and k, the structure of the waves merely changes only for the variation of g, h but here except for the change of direction, the impacts of the values of l, k, m, n are minimal.

The wave profile of the LGH equation

With the assistance of the mathematical program Wolfram Mathematica, the acquired solutions to the LGH equation are picturized in 3D and contour plots with standard values of the related parameters in this sub-section. In general, the results (47)-(49) reflect various forms of solitary waves depending on the wave speed c and the coefficient of the highest power of the nonlinear term of Eq. (37). For the positive values $a = b = 2$ and the negative values $c = -0.06, k = -0.69, \beta = -1.69$, the traveling wave solution (47) depicts a smooth kink soliton. The activation function of the neural networks model with weight k is considered to be the kink soliton in terms of $\tanh(k\lambda)$. Within the limit $-4 \le x, t \le 4$, the 3D and contour profiles have been depicted in Fig. 5 (a).

Similarly, by choosing $a = 1.75, b = -1.6, c = 0.75, k = -0.25, \beta = -1$, the solution (47) yields general sigmoid function revealed in soliton. The 3D and contour profiles have been depicted in Fig. 5(b) within the limit $-5 \le x, t \le 5$. The sigmoid feature is used in the van Genuchten-Gupta model for crop yield response to soil salinity. Sigmoid functions are often used in artificial neural networks for efficiency, are used as wave shaper transfer functions in audio signal processing to simulate the sound of analog circuitry clipping, are used to model. Some sigmoid functions are used in computer graphics and real-time rendering to merge colors or geometry between two values efficiently and without visualization or discontinuities. Due to the logarithmic aspect of the *pH* scale, titration curves between strong acids and strong bases have a sigmoid form.

On the contrary, the negative sign of solution (47) represents a steep kink soliton for the wave speed $c = 0.62$ and the parameters $a = b = -2, k = -0.92, \beta = 0.62$. The 3D and contour profiles have been exhibited in Fig. 6(a) within the limit $-10 \le x, t \le 10$.

The other trigonometric identity of (47) depicts a periodic soliton by expanding the value of the coefficient of nonlinear term $b = -1.31$ with ascending $a = -1.16$ and $k = 0.61$, but descending wave velocity $c = -1.16$ and $\beta = 0.01$. The 3D and contour profiles have been asserted in Fig. 6(b) within the limit $-10 \le x, t \le 10$. Periodic factors such as the influence of environmental factors in mathematical biology, seasonal effects of weather, food supply, mating habits and harvesting, periodicity of parameters are more practical and significant. The study of periodic phenomena occurring in applied problems in technology, natural, and social sciences is the focus of this special solitary wave.

From the estimation (48), we accomplish two distinguish figures when choosing another set of values of c, linear and nonlinear coefficients a, b, wave number β, and weight k involved in Eq (37). With regard to this, considering negative estimation of all $a = -0.10, k = -0.08, b = -0.04, \beta = -1.41$ as well as the wave speed tends to zero i.e., for $c = -0.01$, the result (48) refers to the soliton. Furthermore, when the coefficient of the nonlinear term $b = 1.62$ is increased and different values of $a = -1.92, c = -1.83, k = -0.18, \beta = -1.90$ are used, the absolute value of result (48) shows peaked soliton and is simply called peakon. In Figs. 7(a)-7(b), both the 3D and the contour are exemplified under the constraints $1 \le x, t \le 10$ respectively.

On the other hand, if we accept the negative sign in solution (48), it shows a general soliton shape for the wave velocity $c = 0.28$ and other standards $a = -0.23, b = -0.14, k = -0.06, \beta = -0.14$. The 3D and contour profiles have been depicted after extending the spatial and temporal coordinates within the limit $3 \le x, t \le 20$ in Fig. 8(a). Additionally, with different values of $a = 1.67, b = -0.47, c = -0.3, k = -0.35, \beta = -0.25$, the absolute result $U(x, t)$ in (48) expresses another soliton. The respective 3D and contour profiles have been depicted after attenuating the spatial and temporal coordinates within the limit $1 \le x, t \le 10$ in Fig. 8(b).

Moreover, choosing the positive values of the coefficient $a = 0.77, b = 0.54, c = 0.01, k = 0.11$ but negative $\beta = -2$, the solution (49) shows a flat kink wave shape presenting the 3D and contour profiles in Fig. 9(a) within the boundary $1 \le x, t \le 10$. However, choosing all positive values $a = -0.23, b = -0.23, c = -1.5, k = -1.56, \beta = -1.58$, the solution (49) provides other spike kind soliton of extreme amplitude and ultra-short duration that can be generated in a laser cavity. The 3D and contour profiles have been depicted in Fig. 9(b) within the limit $5 \le x, t \le 50$.

The results, we have established are the hyperbolic and trigonometric solutions for the LGH equation, and the wave profiles are kink, periodic, peakon, sigmoid, spike like solitons, and others. In addition, we have analyzed how the obtained solutions to the LGH equation change the behavior of the waves with respect to the values of related coefficient of the highest power of the linear and nonlinear terms.

Comparison of the results

In this module, the established solutions have been compared with other solutions derived by some other researchers.

Comparison of solutions to the RWEs

Several researchers studied the RWEs using some techniques and obtained some exact solutions, as for example, Peng and Krishnan [34] obtained only two types of rational solutions of sech and tanh functions by choosing the Jacobi elliptic functions in which the periodic waves were derived by the singular manifold scheme. Yong et al. [45] used the generalized expansion technique of the Riccati equation and found non-traveling wave solutions, constant function soliton-like, singular soliton-like solutions, triangular and complex function solutions in terms of hyperbolic and trigonometric structures but there were no traveling wave solutions to describe the interaction of the Riemann wave propagation. Zhang and Meng [47] used the variable separation procedure in which Backlund transformation was set up to build the compacton-anti-compacton and peakon-anti-peakon solitons through trigonometric function solutions only. However, in this study, the extended tanh

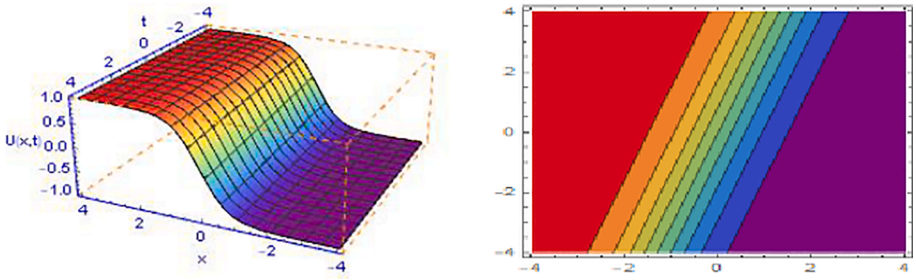

Fig. 5a. Plot of smooth kink wave of solution (49) in terms of $a = 2, b = 2, c = -0.06, k = -0.69, \beta = -1.69$.

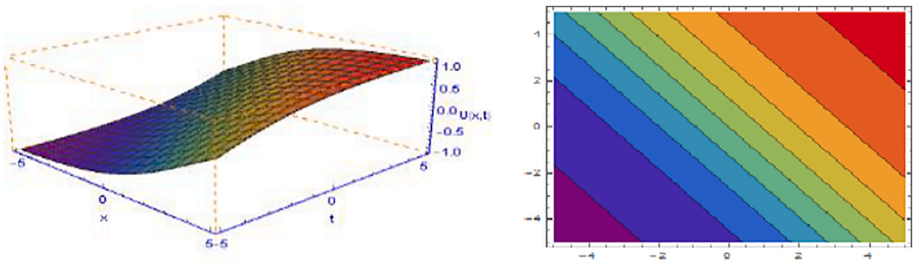

Fig. 5b. Plot of smooth kink wave of solution (47) in terms of $a = 1.75, b = -1.6, c = 0.75, k = -0.25, \beta = -1$.

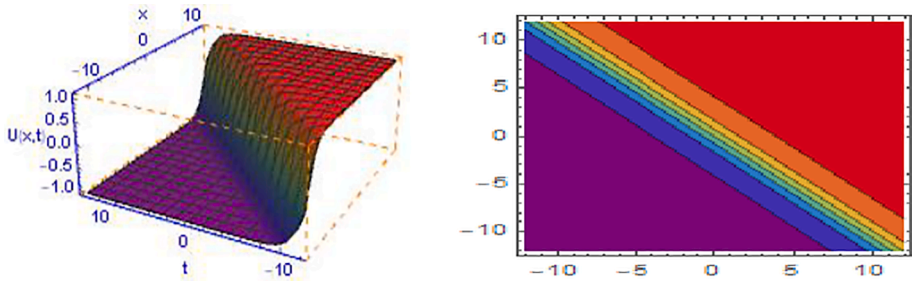

Fig. 6a. Shape of steep kink wave of solution (47) in terms of $a = -2, b = -2, c = 0.62, k = -0.92, \beta = 0.62$.

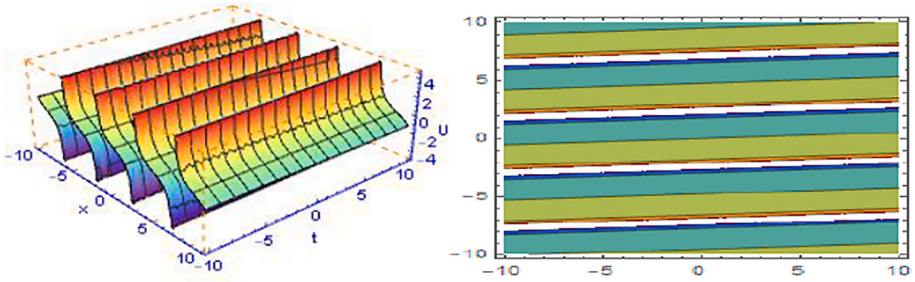

Fig. 6b. Shape of periodic wave of solution (47) in terms of $a = -1.16, b = -1.31, c = -1.16, k = 0.61, \beta = 0.01$.

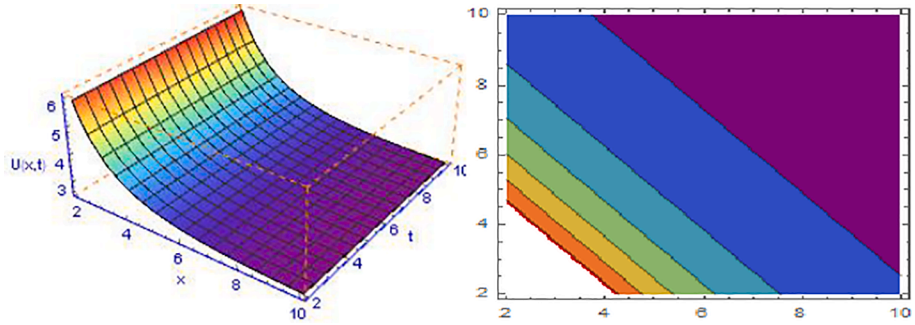

Fig. 7a. Figure of soliton of solution (48) in terms of $a = -0.1, b = -0.04, c = -0.01, k = -0.08, \beta = -1.41$.

scheme covers a wide range of exact traveling wave solutions of RWEs, including tanh, coth, and sech functions, and generates kink, bell-shaped soliton, compacton, parabolic, concave soliton, etc. which was not found earlier. The ascertained results are also graphically presented to examine how a solitary wave propagates with the change of space and time coordinates. In this section, the analytical solutions obtained are compared with the solutions obtained by Jawad et al. [37] with the help of the tanh method in Table 1.

From the above table, it is observed that only sech and tanh functions are found in the solutions determined by Jawad et al. [37]. On the other hand, in the present article, we have established different types of analytic solutions integrating tanh, coth, sech functions that are illustrative, compatible and advanced which internment a sort of evolutionary phenomena.

Comparison of solutions to the LGH equation

The LGH equation has also been studied by means of several techniques and accomplished some exact solutions. For instance, Iftikhar et al. [41] merely established one general solution set of hyperbolic $(\sinh, \cosh)$ and trigonometric $(\sin, \cos)$ functions through $(G'/G, 1/G)$-expansion technique. But there was no explanation about

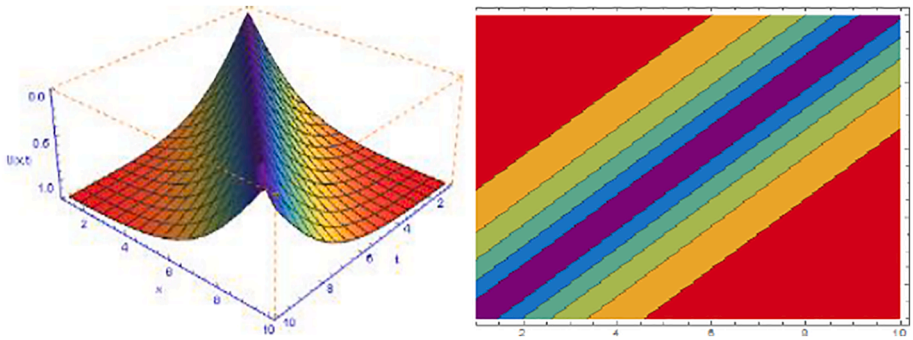

Fig. 7b. Figure of soliton of solution (48) in terms of $a = -1.92, b = 1.62, c = -1.83, k = -0.18, \beta = -1.9$.

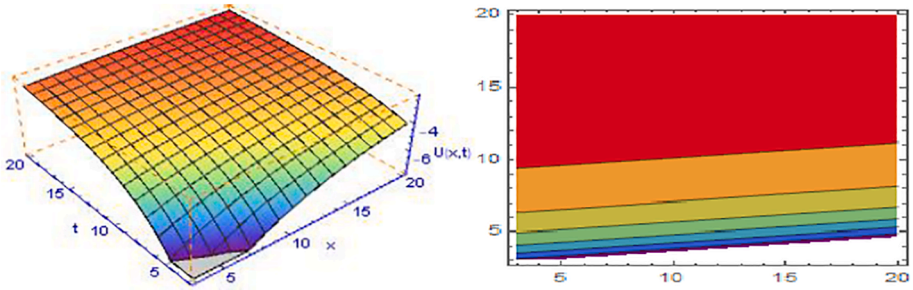

Fig. 8a. General soliton of solution (48) in terms of $a = -0.23, b = -0.14, c = 0.28, k = -0.06, \beta = -0.14$.

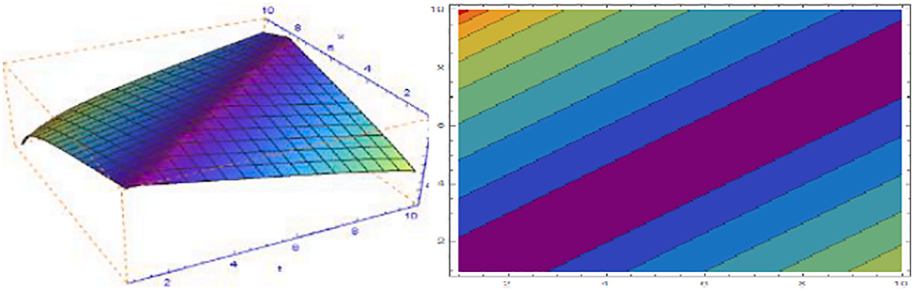

Fig. 8b. General soliton of solution (48) in terms of $a = 1.67, b = -0.47, c = -0.3, k = -0.35, \beta = -0.25$.

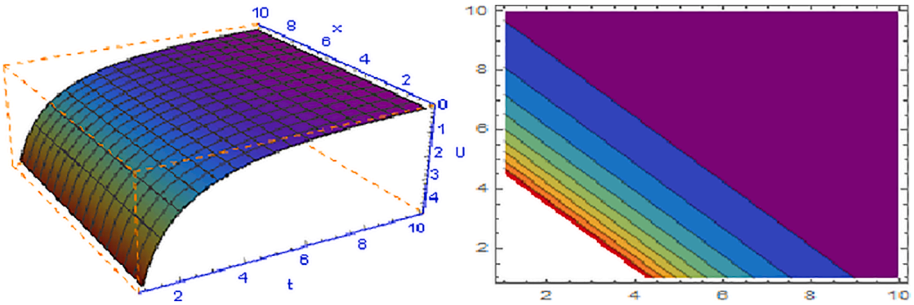

Fig. 9a. Sketched of flat kink of solution (49) in terms of $a = 0.77, b = 0.54, c = 0.01, k = 0.11, \beta = -2$.

the characteristics of the solutions and these solutions possess a few general shapes to describe the traveling waves. Bekir and Unsal [42] determined only two rational solutions with exponential function by employing the first integral method. The behavior of the acquired solutions was not documented there. Cevikel et al. [56] found only the bright and dark solitons using the ansatz solutions $\text{sech}^p\tau$ and $\tanh^p\tau$ respectively through the solitary wave ansatz method. Irshad et al. [57] simply developed some exponential function solutions by the new modified simple equation scheme and obtained only kink, singular kink, and singular periodic shapes. In this article, we have ascertained a variety of hyperbolic function solutions and sketched their shapes, such as, peakon, kink soliton, flat kink soliton, sigmoid as well as some other general solitons which are different from earlier solutions. In this submodule, the attained solutions are compared with Cevikel et al. [56] solutions estimated by the solitary wave ansatz technique in Table 2.

It is noticeable that Cevikel et al. [56] found only two types of

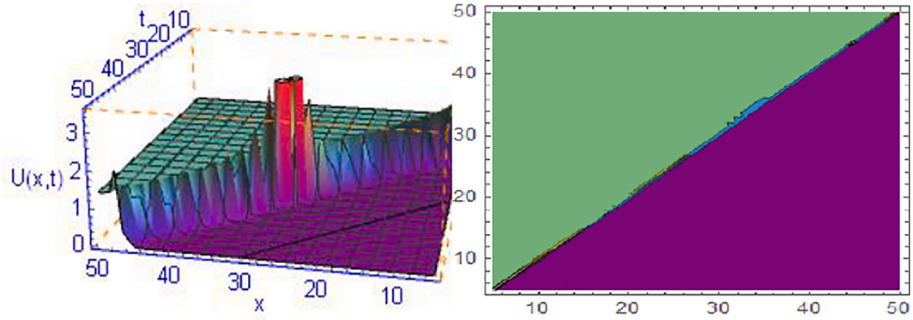

Fig. 9b. Sketched of flat kink of solution (49) in terms of $a = -0.23, b = -0.23, c = -1.5, k = -1.56, \beta = -1.58$.

Table 1
Comparison of the results ascertained by RWEs and results ascertained by Jawad et al. [37]

Jawad et. al. [37] results	Results ascertained in this article
The results (89) and (90) are $g(x,y,t) = A_1 \operatorname{sech}^2(B(B_1x - B_2y - vt))$. $h(x,y,t) = A_2 \operatorname{sech}^2(B(B_1x - B_2y - vt))$. The results (46) and (47) are $u(x,t) = k^2 - \frac{\omega}{8\alpha\beta} - \frac{3}{2\alpha}k^3 \tanh^2(kx + \alpha y + \omega t + \theta_0)$. $v(x,t) = \alpha k - \frac{\omega}{8k\beta} - \frac{3}{2}k^2 \tanh^2(kx + \alpha y + \omega t + \theta_0)$.	The results (30) and (31) are $U(x,y,t) = \frac{12lg^2k^2}{m+n} \operatorname{sech}^2(k(gx + hy - ct))$. $W(x,y,t) = \frac{12hlgk^2}{m+n} \operatorname{sech}^2(k(gx + hy - ct))$. The results (28) and (29) are $U(x,y,t) = -\frac{lg^2k^2}{m+n}\left(20 - 12\operatorname{sech}^2(k(gx + hy - ct)) + 12\coth^2(k(gx + hy - ct))\right)$. $W(x,y,t) = -\frac{hlgk^2}{m+n}\left(20 - 12\operatorname{sech}^2(k(gx + hy - ct)) + 12\coth^2(k(gx + hy - ct))\right)$. The solutions (34) and (35) are $U(x,y,t) = \frac{lg^2k^2}{m+n}\left(4 - 12\coth^2(k(gx + hy - ct))\right)$. $W(x,y,t) = \frac{hlgk^2}{m+n}\left(4 - 12\coth^2(k(gx + hy - ct))\right)$.

Table 2
Comparison of the ascertained results with Cevikel et al. [56]

Cevikel et. al. [56] results	Results ascertained in this article
The result (63) is $u(x,t) = \lambda tanh(\eta(x - vt))$.	The result (49) of this article is $U(x,t) = \pm\frac{a}{b}\tanh(k(\beta x - ct))$.
The result (48) is $u(x,t) = \lambda sech(\eta(x - vt))$.	The result (50) of this article is $U(x,t) = \pm\frac{0.5a}{b}(\tanh(k(\beta x - ct)) + \coth(k(\beta x - ct)))$.

analytic solutions, that is, tanh and sech function solutions. Only the tanh function solution is matched with the solution (47) of the LGH equation and the remaining solutions are diverse. Moreover, the solutions of the present article represent peakon, ideal kink soliton, flat kink soliton, sigmoid, and other soliton shapes which are not portrayed by Cevikel et al. [56].

Conclusions

In this article, we have investigated the nonlinear wave equations, namely the (2 + 1)-dimensional Riemann wave equations and the Landau-Ginsburg-Higgs equation by the aid of the extended tanh method as well as using the solitary wave hypothesis. A variety of explicit traveling wave solutions are established by assigning different particular values of the embodied parameters. The derived results are standard and consistent solitary wave profiles defining by the combination of hyperbolic functions. The established wave estimations might be useful to comprehend nonlinear phenomena, like Landau damping electrostatic waves in plasmas and the electrostatic potential of the ion-cyclotron wave to explain superconductivity and drift coherent ion-cyclotron waves in radially inhomogeneous plasma as well as the ion-acoustic and magneto-sound waves in plasma, and many others wherever there is a research of soliton theory. For the precision of the outcomes, the 3D and contour profiles have been outlined by allocating different parametric preferences. This technique has the advantage of being direct, compatible, and useful in investigating analytical solutions that are significant in discussing nonlinear events in science and engineering. Therefore, the executed technique may be applicable for searching other NLWEs and this is our upcoming work.

CRediT authorship contribution statement

Hemonta Kumar Barman: Conceptualization, Methodology, Software, Resources, Writing - original draft. **Most. Shewly Aktar:** Visualization, Investigation, Data curation. **M. Hafiz Uddin:** Formal analysis, Validation. **M. Ali Akbar:** Project administration, Writing - review & editing, Funding acquisition. **Dumitru Baleanu:** Project administration, Writing - review & editing, Funding acquisition. **M.S. Osman:** Supervision, Writing - review & editing.

Declaration of Competing Interest

The authors declare that they have no known competing financial interests or personal relationships that could have appeared to influence the work reported in this paper.

Acknowledgement

The authors would like to thank the anonymous referees for their insightful comments and suggestions for improving the article.

References

[1] Kallel W, Almusawa H, Mirhosseini-Alizamini SM, Eslami M, Rezazadeh H, Osman MS. Optical soliton solutions for the coupled conformable Fokas-Lenells equation with spatio-temporal dispersion. Results Phys. 2021;26:104388. https://doi.org/10.1016/j.rinp.2021.104388.

[2] Djennadi S, Shawagfeh N, Osman MS, Gómez-Aguilar JF, Arqub OA. The Tikhonov regularization method for the inverse source problem of time fractional heat equation in the view of ABC-fractional technique. Phys. Scr. 2021;96(9):094006.

[3] Akbulut A, Almusawa H, Kaplan M, Osman MS. On the conservation laws and exact solutions to the (3+1)-dimensional modified KdV-Zakharov-Kuznetsov equation. Symmetry. 2021;13(5):765.

[4] Almusawa H, Nur Alam Md, Fayz-Al-Asad Md, Osman MS. New soliton configurations for two different models related to the nonlinear Schrödinger equation through a graded-index waveguide. AIP Adv. 2021;11(6):065320. https://doi.org/10.1063/5.0053565.

[5] Osman MS, Baleanu D, Adem AR, Hosseini K, Mirzazadeh M, Eslami M. Double-wave solutions and Lie symmetry analysis to the (2+1)-dimensional coupled Burgers equations. Chin. J. Phys. 2020;63:122–9.

[6] Apel JR, Ostrovsky LA, Stepanyants YA, Lynch JF. Internal solitons in the ocean and their effect on underwater sound. J. Acoust. Soc. Am. 2006;121(2):695–722.

[7] Wazwaz A-M. A new integrable (2+1)-dimensional generalized breaking soliton equation: N-soliton solutions and traveling Wave Solutions. Commun. Theor. Phys. 2016;66(4):385–8.

[8] Yaqub Khan M, Iqbal J. Effect of entropy on soliton profile in ITG driven magneto-plasma. Phys Plasmas 2017;24(8):082514. https://doi.org/10.1063/1.4989895.

[9] Hietarinta J. Hirota's bilinear method and soliton solutions. Phys. AUC 2005;15:31–7.

[10] Akbar MA, Lanre A, Yao SW, Jhangeer A, Rezazadeh H, Khater MMA, et al. Soliton solutions to the Boussinesq equation through sine-Gordon method and Kudryashov method. Results Phys. 2021;25(104228):1–10.

[11] Liu J-G, Osman MS, Wazwaz A-M. A variety of nonautonomous complex wave solutions for the (2+ 1)-dimensional nonlinear Schrödinger equation with variable coefficients in nonlinear optical fibers. Optik. 2019;180:917–23.

[12] Akinyemi L, Rezazadeh H, Yao S-W, Akbar MA, Khater MMA, Jhangeer A, et al. Nonlinear dispersion in parabolic law medium and its optical solitons. Results Phys. 2021;26:104411. https://doi.org/10.1016/j.rinp.2021.104411.

[13] Gurefe Y, Misirli E. Exp-function method for solving nonlinear evolution equations with higher order nonlinearity. Comput. Math. Appl. 2011;61:2025–30.

[14] Ali KK, Cattani C, Gómez-Aguilar JF, Baleanu D, Osman MS. Analytical and numerical study of the DNA dynamics arising in oscillator-chain of Peyrard-Bishop model. Chaos Soliton Fract. 2020;139:110089. https://doi.org/10.1016/j.chaos.2020.110089.

[15] Khan K, Akbar MA, Islam MH, Salam MA. A note on enhanced (G'/G)-expansion method in nonlinear physics. Ain Shams. Engg. J. 2014;5:877–84.

[16] Lin L, Zhu S, Xu Y, Shi Y. Exact solutions of Gardner equations through Tanh-Coth method. Appl. Math. 2016;7:2374–81.

[17] Akbar MA, Ali NM. The improved F-expansion method with Riccati equation and its application in mathematical physics. Cogent Math. 2017;4(1):282–577.

[18] Yokus A, Bulut H. On the numerical investigations to the Cahn-Allen equation by using finite difference method. Int. J. Optimization Cont.: Theo. Appl. 2018;9:18–23.

[19] Torlak M, Hadziabdic V. Solving linear wave equation using a finite-volume method in time domain on unstructured computational grids. Lecture Notes in Networks and Systems 2018;2018:347–56.

[20] Kumar D, Seadawy AR, Joardar AK. Modified Kudryashov method via new exact solutions for some conformable fractional differential equations arising in mathematical biology. Chin. J. Phys. 2018;56(1):75–85.

[21] Gundogdu H, Gozukızıl OF. On different kinds of solutions to simplified modified form of a Camassa-Holm equation. J. Appl. Math. Comput. Mech. 2019;18(2):31–40.

[22] Li W, Pang Y. Application of Adomian decomposition method to nonlinear systems. Adv. Differ. Equ. 2020;2020:67.

[23] Islam ME, Barman HK, Akbar MA. Search for interactions of phenomena described by the coupled Higgs field equation through analytical solutions. Opt. Quantum. Electron. 2020;52:468.

[24] Kayum MA, Ara S, Osman MS, Akbar MA, Gepreel KA. Onset of the broad-ranging general stable soliton solutions of nonlinear equations in physics and gas dynamics. Results Phys. 2021;20:103762. https://doi.org/10.1016/j.rinp.2020.103762.

[25] Ghanbari B, Nisar KS, Aldhaifallah M. Abundant solitary wave solutions to an extended nonlinear Schrodinger's equation with conformable derivative using an efficient integration method. Adv. Differ. Equ. 2020;2020:328.

[26] Ghanbari B, Yusuf A, Inc M, Baleanu D. The new exact solitary wave solutions and stability analysis for the (2 + 1)-dimensional Zakharov-Kuznetsov equation. Adv. Differ. Equ. 2019;2019:49.

[27] Ghanbari B, Inc M, Rada L. Solitary wave solutions to the Tzitzeita type equations obtained by a new efficient approach. J. Appl. Anal. Comput. 2019;9(2):568–89.

[28] M. Srivastava H, Günerhan H, Ghanbari B. Exact traveling wave solutions for resonance nonlinear Schrödinger equation with intermodal dispersions and the Kerr law nonlinearity. Math. Methods Appl. Sci. 2019;42(18):7210–21. https://doi.org/10.1002/mma.v42.1810.1002/mma.5827.

[29] Ghanbari B. On the nondifferentiable exact solutions to Schamel's equation with local fractional derivative on Cantor sets. Numer. Methods Partial Differ. Equ. 2020. https://doi.org/10.1002/num.22740.

[30] Ghanbari B. On novel nondifferentiable exact solutions to local fractional Gardner's equation using an effective technique. Math. Methods Appl. Sci. 2021;44(6):4673–85. https://doi.org/10.1002/mma.v44.610.1002/mma.7060.

[31] Munusamy K, Ravichandran C, Nisar KS, Ghanbari B. Existence of solutions for some functional integrodifferential equations with nonlocal conditions. Math. Methods Appl. Sci. 2020;43(17):10319–31. https://doi.org/10.1002/mma.v43.1710.1002/mma.6698.

[32] Ghanbari B. Abundant exact solutions to a generalized nonlinear Schrödinger equation with local fractional derivative. Math. Methods Appl. Sci. 2021;44(11):8759–74. https://doi.org/10.1002/mma.v44.1110.1002/mma.7302.

[33] Radha R, Laksmanan M. Dromion like structures in the (2+1)-dimensional breaking soliton equation. Phys. Lett. A 1995;197:7–12.

[34] Peng YZ, Krishnan EV. Two classes of new exact solutions to (2+1)-dimensional breaking soliton equation. Commun. Theor. Phys. 2005;44(5):807–9.

[35] Bogoyavlensky IO, Nauk IA SSSR, Ser. Mat. 53(1989): 243, 907; IBID. 54 (1990) 123.

[36] Xu G-Q. Integrability of a (2+1)-dimensional generalized breaking soliton equation. Appl. Math. Lett. 2015;50:16–22.

[37] Jawad AJM, Johnson S, Yildirim A, Kumar S, Biswas A. Soliton solutions to the coupled nonlinear wave equations in (2 + 1) dimensions. Indian J. Phys. 2013;87(3):281–7.

[38] Spatschek KH, Shukla PK. Nonlinear interaction of magneto-sound wave with whistler turbulence. Radio Sci 1978;13(1):211–4.

[39] Khuri SA. Exact solutions for a class of nonlinear evolution equations: A unified ansätze approach. Chaos, Soliton. Fract. 2008;36(5):1181–8.

[40] Chen Y, Li B, Zhang H. Exact solutions for a new class of nonlinear evolution equations with nonlinear term of any order. Chaos, Soliton. Fract. 2003;17:675–82.

[41] Iftikhar A, Ghafoor A, Zubair T, Firdous S, Mohyud-Din ST. G'G,1G-expansion method for traveling wave solutions of (2 + 1) dimensional generalized KdV, Sin Gordon and Landau-Ginzburg-Higgs equations. Sci. Res. Essays 2013;8(28):1349–59.

[42] Bekir1 A, Unsal O.. Exact solutions for a class of nonlinear wave equations by using First Integral Method. Int. J. Nonlinear Sci. 2013;15(2):99–110.

[43] Cyrot M. Ginzburg-Landau theory for superconductors. Rep. Prog. Phys. 1973;36(2):103–58.

[44] Ruan H-yu. On the coherent structures of (2+1)-dimensional breaking soliton equation. J. Phys. Soc. Japan 2002;71(2):453–7.

[45] Yong C, Biao L, Qing ZH. Symbolic computation and construction of soliton-like solutions to the (2+1)-dimensional breaking soliton equation. Commun. Theor. Phys. 2003;40(2):137–42.

[46] Yan-Ze P. New exact solutions for (2+1)-dimensional breaking soliton equation. Commun. Theor. Phys. 2005;43(2):205–7.

[47] Zhang JF, Meng JP. New localized coherent structures to the (2+1)-dimensional breaking soliton equation. Phys. Lett. A 2004;321:173–8.

[48] Ren YZ, Liu ST, Zhang HQ. On a Generalized Extended *F* -Expansion Method. Commun. Theor. Phys. 2006;45(1):15–28.

[49] Barman HK, Seadawy AR, Ali Akbar M, Baleanu D. Competent closed form soliton solutions to the Riemann wave equation and the Novikov-Veselov equation. Results in Phys. 2020;17:103131. https://doi.org/10.1016/j.rinp.2020.103131.

[50] Bai C. Exact solutions for nonlinear partial differential equation: a new approach. Phys. Lett. A 2001;288:191–5.

[51] Elwakil SA, El-labany SK, Zahran MA, Sabry R. Modified extended tanh-function method for solving nonlinear partial differential equations. Phys. Lett. A 2002;299:179–88.

[52] Li P, Pan Z. A new development on Jacobian elliptic function expansion method. Phys. Lett. A 2004;332:39–48.

[53] Xie F, Gao X. Exact travelling wave solutions for a class of nonlinear partial differential equations. Chaos Soliton. Fract. 2004;19:1113–7.

[54] Darwish AA, Ramady A. Applications of algebraic method to exactly solve some nonlinear partial differential equations. Chaos Soliton. Fract. 2007;33:1263–74.

[55] Hu WP, Deng ZC, Han SM, Fan W. Multi-symplectic Runge-Kutta methods for Landau-Ginzburg-Higgs equation. Appl. Math. Mech. -Engl. Ed. 2009;30(8):1027–34.

[56] Cevikel AC, Aksoy E, Guner O, Bekir A. Dark-Bright soliton solutions for some evolution equations. Int. J. Nonlinear Sci. 2013;16(3):195–202.

[57] Irshad A, Mohyud-Din ST, Ahmed N, Khan U. A new modification in simple equation method and its applications on nonlinear equations of physical nature. Results Phys. 2017;7:4232–40.

[58] Islam ME, Akbar MA. Stable wave solutions to the Landau-Ginzburg-Higgs equation and the modified equal width wave equation using the IBSEF method. Arab. J. Basic Appl. Sci. 2020;27(1):270–8.

[59] Barman HK, Akbar MA, Osman MS, Nisar KS, Zakarya M, Abdel-Aty A-H, et al. Solutions to the Konopelchenko-Dubrovsky equation and the Landau Ginzburg-Higgs equation via the generalized Kudryashov technique. Results Phys. 2021;24:104092. https://doi.org/10.1016/j.rinp.2021.104092.

[60] Kundu PR, Almusawa H, Fahim MRA, Islam ME, Akbar MA, Osman MS. Linear and nonlinear effects analysis on wave profiles in optics and quantum physics. Results Phys. 2021;23:103995. https://doi.org/10.1016/j.rinp.2021.103995.

[61] Wazwaz A-M. The extended tanh method for new solitons solutions for many forms of the fifth-order KdV equations. Appl. Math. Comput. 2007;184(2):1002–14.

[62] Wazwaz AM. The extended tanh method for abundant solitary wave solution of nonlinear wave equations. Appl. Math. Comput. 2007;187:1131–42.